BIOCHEMISTRY
including biophysical chemistry & molecular biology

Article

pubs.acs.org/biochemistry

Intrinsically Disordered N-Terminus of Calponin Homology-Associated Smooth Muscle Protein (CHASM) Interacts with the Calponin Homology Domain to Enable Tropomyosin Binding

Justin A. MacDonald,[*,†] Hiroaki Ishida,[#,‡] Eric I. Butler,[#,†] Annegret Ulke-Lemée,[#,†] Mona Chappellaz,[†] Sarah E. Tulk,[†] John K. Chik,[§] and Hans J. Vogel[‡]

[†]Department of Biochemistry & Molecular Biology, University of Calgary, 3280 Hospital Drive NW, Calgary, Alberta, Canada T2N 4Z6

[‡]Department of Biological Sciences, University of Calgary, 2500 University Drive NW, Calgary, Alberta, Canada T2N 4N1

[§]Department of Chemical & Biological Sciences, Mount Royal University, 4825 Mount Royal Gate NW, Calgary, Alberta, Canada T3E 6K6

Supporting Information

ABSTRACT: The calponin homology-associated smooth muscle (CHASM) protein plays an important adaptive role in smooth and skeletal muscle contraction. CHASM is associated with increased muscle contractility and can be localized to the contractile thin filament via its binding interaction with tropomyosin. We sought to define the structural basis for the interaction of CHASM with smooth muscle tropomyosin as a first step to understanding the contribution of CHASM to the contractile capacity of smooth muscle. Herein, we provide a structure-based model for the tropomyosin-binding domain of CHASM using a combination of hydrogen/deuterium exchange mass spectrometry (HDX-MS) and NMR analyses. Our studies provide evidence that a portion of the N-terminal intrinsically disordered region forms intramolecular contacts with the globular C-terminal calponin homology (CH) domain. Ultimately, cooperativeness between these structurally dissimilar regions is required for CHASM binding to smooth muscle tropomyosin. Furthermore, it appears that the type-2 CH domain of CHASM is required for tropomyosin binding and presents a novel function for this protein domain.

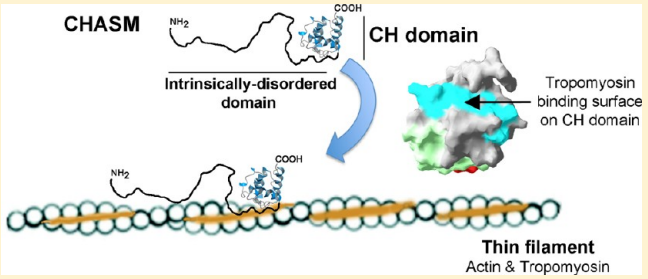

The calponin homology-associated smooth muscle (CHASM) protein,[1] also called smoothelin-like 1 (SMTNL1), belongs to the smoothelin family of muscle proteins. The smoothelins are a family of cytoskeletal proteins specifically expressed in, and frequently used as markers of, differentiated contractile smooth muscle cells.[2] Knowledge pertaining to their physiological function remains limited; however, it appears that smoothelins may lock smooth muscle cells in a contractile phenotype, possibly by regulating and stabilizing contractile structures.[3] Thus, it is significant that genetic deletion of smoothelin-A,[4] smoothelin-B,[5] and CHASM[6] have been linked with decreased contractile potential, and all three proteins have been identified to colocalize with contractile filaments.[3,7−10] The CHASM protein promotes an exaggerated vascular contractile phenotype. In its presence, vascular aortic smooth muscle was more responsive to contractile agonists and less responsive to relaxant agonists.[6] Studies have also implicated the CHASM protein in mediating cardiovascular adaptations to exercise[6] as well as development and pregnancy.[11,12] CHASM expression increased dramatically as mice progress through sexual development, while endurance exercise and pregnancy contributed to reduce CHASM expression. Thus, current knowledge suggests an important role for CHASM in the modulation of vascular smooth muscle contractile activity.

It would appear that the mechanism(s) responsible for the interaction with the contractile apparatus differs among the different smoothelin family members. In this context, CHASM is unable to bind directly to F-actin filaments[13] and appears to associate with contractile filaments via a tropomyosin-binding domain.[10] This binding mechanism is distinct from that of the smoothelins, which seem to associate with filamentous actin via the dual participation of a C-terminal, type-2 calponin homology (CH) domain and other undefined regions of the protein.[7,9] There are five defined CH domain subtypes that display a large degree of structural conservation (reviewed in ref 14); however, the individual subtypes display quite striking functional variability. While the C-terminus of the CHASM protein also contains a type-2 CH domain (residues 342−459), this region is unable to promote F-actin binding.[1] Regardless, our recent studies have revealed that the CH domain of CHASM is integral to several functional properties of the

Received: December 20, 2011
Revised: March 14, 2012
Published: March 16, 2012

dx.doi.org/10.1021/bi2019018 | *Biochemistry* 2012, 51, 2694−2705

protein, including a unique association with apo-calmodulin,[15] effects on the ability of smooth muscle to relax ex vivo,[13] and tropomyosin-binding and localization to contractile filaments in smooth muscle cells.[10] Furthermore, the N-terminus (residues 1−341) of CHASM, composed of entirely unique sequence and thought to possess intrinsic structural disorder, is also viewed as having important, functional properties, including binding domains for the progesterone receptor[12] and tropomyosin.[10]

Tropomyosin serves essential structural and functional roles in smooth muscle filaments.[16,17] Notably, the protein is localized to the F-actin thin filament, essentially forming a continuous polymer along each of the two major grooves in the F-actin polymer, and contributes to the regulation and stabilization of the thin filament assembly. Current evidence supports a role for tropomyosin in coordinating the structure of actin monomers within the filament to enable myosin−actin interactions, as well in regulating general thin filament stability,[17] so it is not surprising that the association of proteins to actin and/or tropomyosin may dynamically influence the actin filament structure. We have previously demonstrated with a variety of binding assays that the interaction of CHASM with tropomyosin was dependent on the presence of the CH domain as well as a portion of the intrinsically disordered N-terminus.[10] However, the structural disorder associated with CHASM has prevented a precise molecular definition of the interaction interface. Here, we utilize a combination of NMR and hydrogen/deuterium-exchange mass spectrometry (HDX-MS) to identify intramolecular associations between the CH domain and intrinsically disordered N-terminal extension of CHASM (herein referred to as the IDR) that stabilize the domain and provide a favorable interface for the binding of tropomyosin. As such, the data reported in this study provide a refinement of the structural basis for the CHASM interaction with tropomyosin.

EXPERIMENTAL PROCEDURES

Materials. Smooth muscle tropomyosin, purified from chicken gizzard and composed of α- and β-isoforms, was kindly provided by Dr. Michael Walsh (University of Calgary). Precission protease, pGEX-6P1, and glutathione-Sepharose 4B were from GE Healthcare (Piscataway, NJ). $^{15}NH_4Cl$ was from Cambridge Isotopes (Andover, MA). Porozyme-immobilized pepsin was obtained from Applied Biosystems (Carlsbad, CA).

Expression and Purification of Recombinant CHASM Proteins. The full-length CHASM gene (*Mus musculus*; GenBank ID: EDL27304.1) was obtained from IMAGE clone 3593616 (Research Genetics).[1] The calponin homology (CH) domain and tropomyosin-binding region (TMB) of CHASM were amplified by standard PCR techniques (CHASM-CH, bp 1036−1380/aa 346−459 and CHASM-TMB, bp 583−1380/aa 195−459) and subcloned into the pGEX-6P1 vector that provided an N-terminal glutathione-*S*-transferase (GST) tag. The proximal portion of the N-terminal intrinsically disordered region (CHASM-pxIDR, bp 585−1035/aa 195−345) was also cloned, expressed, and purified as described previously.[10] The various constructs were verified by DNA sequencing, and then GST-fusion proteins were produced in *Escherichia coli* BL21 (DE3) in LB media. The resultant GST-fusions were purified with glutathione-Sepharose resin and were cleaved "on-column" with PreScission Protease. The eluted proteins contained the cloning artifact "GPLGS" at their N-terminus. The concentration of each CHASM protein was determined using its predicted molar extinction coefficient (cm^{-1} M^{-1}): CHASM-CH, ε_{280} = 18450; CHASM-pxIDR, ε_{280} = 5500; and CHASM-TMB, ε_{280} = 23950.

NMR Sample Preparation. Standard protocols were used to generate uniformly ^{15}N-enriched CHASM-CH and CHASM-TMB proteins for NMR experiments. Transformed bacteria were grown in M9 minimal media containing 0.5 g/L $^{15}NH_4Cl$ and unlabeled glucose. The CHASM proteins were concentrated and exchanged into 1 mM sodium phosphate buffer with a centrifugal filter device. All NMR spectra were obtained at 20 °C on a Bruker Avance 500 MHz NMR spectrometer equipped with a triple resonance inverse Cryoprobe with a single *z*-axis gradient. The [^1H, ^{15}N]-HSQC spectrum of CHASM-CH and the resonance assignments were obtained from Ishida et al. (PDB ID: 2JV9[15]). NMR samples contained approximately 0.3 mM uniformly ^{15}N-labeled CHASM-TMB or CHASM-CH protein, 20 mM Bis-Tris buffer (pH 6.8), 50 mM KCl, 5 mM dithiothreitol, and 0.5 mM 2,2-dimethyl-2-silapentane-5-sulfate. The [^1H, ^{15}N]-HSQC spectra of ^{15}N-CHASM-CH were acquired in the presence and absence of CHASM-pxIDR to examine the intramolecular interactions of the CH domain and the central core region. The chemical shift perturbation (CSP) studies were performed by monitoring the ^1H, ^{15}N HSQC spectra of ^{15}N-labeled CHASM-CH with the addition of unlabeled CHASM-pxIDR. The CSP value was then evaluated as a weighted average chemical shift difference of ^1H and ^{15}N resonances, using the equation $CSP = \sqrt{(\Delta HN)^2 + (\Delta N/5)^2}$.[18] Chemical shifts in all spectra were referenced using 2,2-dimethyl-2-silapentanesulfonic acid to obtain ^1H, ^{15}N chemical shifts.[19] In additional experiments, the [^1H, ^{15}N]-HSQC spectra of CHASM-TMB were acquired in the presence and absence of tropomyosin. Approximately 1.7 mol equiv of unlabeled tropomyosin (with respect to the CHASM-TMB content) was added into the NMR sample. The concentration of tropomyosin was determined using the Bradford protein assay with bovine serum albumin as the standard. All spectra were processed using NMRPipe[20] and analyzed using the NMRView software.[21]

CD Spectroscopy. CD spectra were acquired on a Jasco J-810 spectropolarimeter (Jasco Inc., Easton MD) as defined previously.[22] Briefly, all experiments were measured from 260 to 190 nm at ambient temperature (22 °C) in a 1 mm path length cuvette using the following parameters averaged over 10 scans: 0.5 nm step resolution, 100 nm/min speed, 0.5 s response time, and 1 nm bandwidth. Each sample contained 5 μM of protein in 20 mM potassium phosphate buffer, pH 7.0. The background signals from the buffer were subtracted, and then the data were converted to mean residue ellipticity.

Tropomyosin-Sepharose Pull-Down Assays. Four nanomoles of purified CHASM-CH, CHASM-pxIDR, CHASM-TMB as well as CHASM-CH plus CHASM-pxIDR together were incubated with molar excess tropomyosin-Sepharose (10 mM α/β-tropomyosin immobilized to Sepharose as described in ref 10) in 500 μL of binding buffer (25 mM Tris-HCl, pH 7.4, 10 mM NaCl) for 1 h at 4 °C with rotating. The beads were collected by centrifugation and washed with 1.5 mL of binding buffer five times. Captured CHASM proteins were then eluted in SDS buffer (20 μL) and analyzed by SDS−PAGE with Coomassie staining. The amount of CHASM protein bound to tropomyosin-Sepharose was compared to that captured on blank-Sepharose.

Sample Preparation for Hydrogen−Deuterium Exchange Mass Spectrometry (HDX-MS). Proteins were

dx.doi.org/10.1021/bi2019018 | *Biochemistry* 2012, 51, 2694−2705

dialyzed into 25 mM Tris-HCl, pH 7.2 and 25 mM NaCl. CHASM protein samples (5 mg/mL) for binding experiments were mixed in a 1:2 molar ratio with binding partners to ensure saturation and incubated for 10 min prior to HDX-MS analysis. Protein samples were automatically mixed with a WPS-3000 autosampler prior to injection on an Ultimate 3000 HPLC operated by Chromeleon 6.7 software (Dionex, Bannockburn, IL). In a typical HDX analysis, an aliquot (10.2 μL) of CHASM protein was mixed with heavy water (D_2O, 3.4 μL) at 23 °C and after 30 s, 0.3 M glycine-HCl, pH 2.2 (6.8 μL) was added to quench the exchange. The mixture was immediately loaded onto an HPLC via a 20 μL loading loop and injected with a flow rate of 40 μL/min over a self-packed, immobilized pepsin column (40 μL bed volume; Applied Biosystems) at 23 °C. After digestion (~1 min), peptides were captured on a C-8 Bruker-Michrom MicroTrap column in a refrigerated 4 °C unit. At this point, the flow direction on the C-8 trap column was reversed with a new flow rate (5 μL/min) and mobile phase (5% ACN, 0.05% TFA). The eluted sample peptides were captured on a C-18 separation column (Phenomenex Jupiter 5 μm 300 Å C-18, 50 × 1 mm) held at 4 °C and eluted over 20 min with an ACN gradient (20−50% ACN in 0.05% TFA).

Tandem Mass Spectrometry Identification of Peptide Fragments. Peptides eluting from the HPLC were passed directly by electrospray ionization to a QTrap API 2000 mass spectrometer (Applied Biosystems, Foster City, CA). Ions were initially scanned by enhanced mass spectrum (EMS) over a range of 300−1060 m/z. Ions with charge state z = 1 or 2 and intensity over 10^5 counts were additionally submitted for enhanced resolution (ER) scan at a lower scan speed and higher resolution to confirm charge state and isotope pattern. Peptides with a charge of 1 or 2 were submitted for tandem MS/MS analysis by enhanced product ion (EPI) scan with a rolling collision energy capped at 80 eV. The resultant MS/MS spectra were converted to universal mzML format using MSConvert (ProteoWizard, open source software) and then analyzed with the Trans-Proteomics Pipeline (TPP) software package (Seattle Proteome Center; open source software). The X!Tandem peptide assignment protocol (Global Proteome Machine Organization) was applied to the mzML peak list to predict identification of peptides from the MS/MS data. A FASTA database containing the sequences of the CHASM and tropomyosin, in addition to an extensive list of human and mouse keratins and other possible contaminants (e.g., GST, keratin, precission protease, actin, and myosin) was used for peak assignation. Any amino acid was considered a possible cut site due to the wide range of possible pepsin cleavages. Methionine oxidation and cysteine carbamido-methylation were allowed as possible modifications to amino acids, though only oxidation of methionine was detected. The database of peptides assigned by X!Tandem was converted to pepXML format using the bundled Tandem2XML software (Seattle Proteome Center). Peptide lists were then submitted to PeptideProphet (Institute for Systems Biology, Seattle; open source software) for validation. Peptides with a probability score lower than 0.5 or a chain-length less than five amino acid residues were removed from the analysis.

Calculation of Hydrogen−Deuterium Exchange and Statistical Analysis. The mass spectrum of each peptide as identified by the TPP software was extracted and checked for abnormalities (e.g., the presence of coeluting species) that might interfere with the analysis. The weighted average m/z ($m/z_{w.avg}$) of each clean spectrum was calculated by multiplying the m/z of each peak in a mass envelope by the overall portion of that peak's intensity compared to the sum intensity of all peaks in the envelope using the following formula. The calculated m/z of the spectrum was subtracted from the $m/z_{w.avg}$, multiplied by the charge of the ion (1 or 2), and finally divided by the deuterium percent (25%) to calculate the "gross hydrogen deuterium exchange (HDX)", the overall change in mass with the introduction of deuterium. To obtain a final percent hydrogen−deuterium exchange (%HDX), the gross exchange was divided by the number of amino acid residues in the peptide that were capable of exchange (i.e., all residues except proline). The weighted mass was compared to the theoretical m/z of the peptide, not to the mass obtained experimentally, and therefore, is an index value. The %HDX values are expressed as the weighted average percent exchange plus or minus the standard deviation of the average. Statistical significance was calculated using the Student's t test (2-tailed) with $p < 0.05$ considered to be significant.

Structural Modeling. The three-dimensional (3D) structure of the CHASM CH domain as determined by NMR (PDB ID: 2JV9) was downloaded from NCBI and imported into PyMOL.[23] The amino acid sequence of the pxIDR was added manually using the PyMOL software's built-in protein sequence generator and sculpting tools.

RESULTS

In Silico Structure Analysis of the CHASM N-Terminal Region. For the purpose of this study, the entire sequence located amino-terminal to the CH domain (i.e., residues Met-1 to Lys-346) was considered to be the N-terminal intrinsically disordered region (IDR) of the CHASM protein. This sequence consists of clusters of basic and acidic amino acids distributed throughout the entire region. Inspection of the IDR of CHASM revealed distinct differences in net charge and pI as well as proline and hydrophobic amino acid content when compared to the CH domain. The IDR had a pI of 4.3 while the CH domain had a pI of 8.9. The IDR possesses very little aromatic amino acid content when compared with the CH domain, 1% and 11%, respectively, and considerably less hydrophobic amino acid content, 11% in the IDR and 25% in the CH domain. In addition, the proline content of the IDR sequence is considerably higher, 9.0% versus 2.9%. The first ~250 amino acids of CHASM contain 11/26 total proline residues, and the last ~150 amino acids contain only 3/26 proline residues. Moreover, there is also a marked change in proline content in the sequence surrounding the Ser-301 phosphorylation site, with this region (i.e., 251−310) containing 12/26 or ~46% of the total proline residues. The high content of proline residues in this region may have some implication for the biochemical function of CHASM, since high proline content is an indication of structural disorder with proline residues conferring significant conformational restraints.[24]

The CHASM sequence was analyzed in silico for disorder using DISOPRED,[25] and secondary structure content was analyzed using PSIPRED[26] and UNIPROT.[27] The results of DISOPRED analysis suggest residues (1−338) present in the IDR of CHASM to be intrinsically disordered (Figure 1A). Indeed, a previous report suggested that there was little structure obtained for the N-terminal region of CHASM when preliminary examinations were completed with circular dichroism (CD) and NMR.[6] Secondary structure predictors such as PSIPRED and UNIPROT suggested mostly α-helical

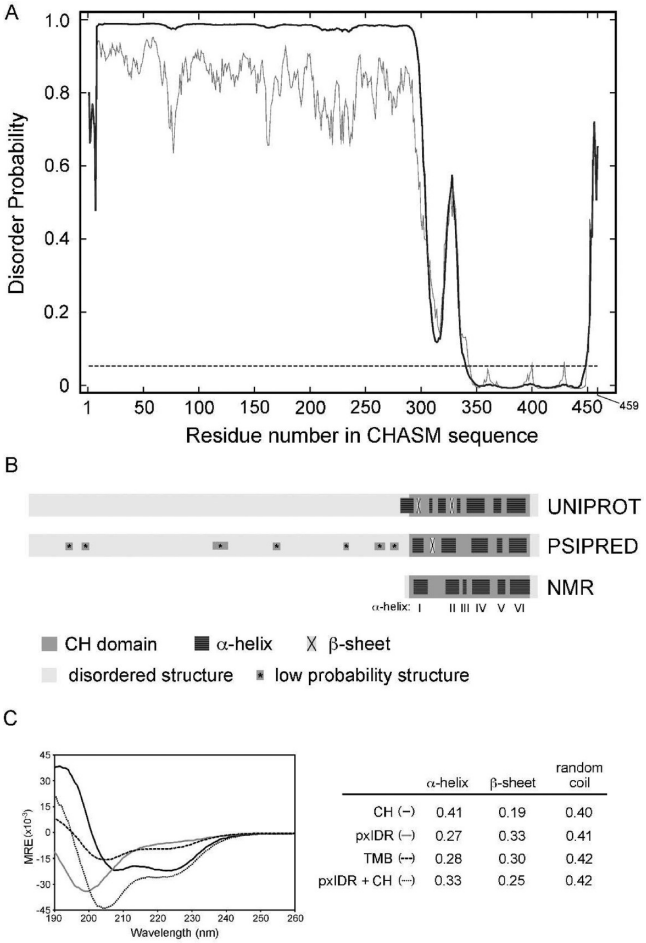

Figure 1. Bioinformatic and biophysical analyses of the CHASM protein for disorder and secondary structure predictions. Residues 1–459 of the full-length CHASM protein are indicated. In (A), regions of disorder were predicted with DISOPRED2. Calculated results are represented by the thin gray line, and results obtained following passage through a 2% false positive filter are represented by the heavy black line. The 5% confidence interval is represented by the dashed-line; any amino acid residue found below this interval is assumed to be associated with an ordered structure. Secondary structures were predicted in (B) with UNIPROT or PSIPRED programs. PSIPRED ranks predicted structures on a 0–9 scale; only structures of likelihood 5 or greater are depicted. Low probability structures (with scores <7) are marked with an asterisk (*). The secondary structure of the isolated CH domain with defined α-helices as determined by NMR[15] is also presented. In (C), far-UV CD spectra of CHASM-CH (solid line), CHASM-pxIDR (solid gray line), CHASM-TMB (dashed line) as well as the CHASM-pxIDR-CH complex (dotted line) are shown. The CD intensities are expressed as the mean residue molar ellipticity.

content for the CH domain with little structure predicted for the IDR (Figure 1B). This is in agreement with a solution structure for the CH domain of CHASM generated from previously completed NMR experiments,[15] and PSIPRED did predict the major α-helices of the CH domain with some degree of accuracy so long as only high-scoring results (greater than 7 on a 0–9 confidence scale) were considered. In addition, the C-terminal "tail" sequence (449–459) of CHASM was predicted to possess significant disorder. Most interestingly, there was suggestion of some structural order (Figure 1A,B) in the proximal region of the IDR that resides next to the CH domain. DISOPRED predicted a possible spike in structural order at a 20% confidence interval, around residues 313–318. We next examined the secondary structure of the CH domain and pxIDR by far-UV CD spectroscopy. The CH domain itself contains a high amount of α-helix, as one might expect based on the previous NMR structural solution,[15] while the CHASM-pxIDR and CHASM-TMB polypeptides possessed less α-helical content (Figure 1C). It should be noted that there were no large differences in spectroscopic features observed when the far-UV CD of CHASM-TMB was compared with CHASM-CH plus CHASM-pxIDR. These results imply that α-helical structure was not induced in the pxIDR upon interaction with the CH domain, although minor structural alterations may not be detectable with this method. Overall, our analyses are suggestive of potential structure within the pxIDR that could provide an intramolecular interface between the globular CH domain and intrinsically disordered N-terminal region.

NMR Studies Define Intramolecular Interactions between the CH Domain and Intrinsically Disordered Region. Previous data reveal that the IDR is required for the interaction of CHASM with tropomyosin.[10] The interaction surface may extend over ~150 residues to include undefined portions of the pxIDR located immediately adjacent to the CH domain as well as the CH domain itself. We undertook an NMR analysis of the CHASM-TMB construct to define the contribution of the CH domain and pxIDR sequence to the tropomyosin interaction. In Figure 2A, the [^{1}H, ^{15}N]-HSQC spectrum of CHASM-TMB was superimposed on the previously assigned spectrum for the isolated CHASM-CH protein.[15] The majority of the dispersed signals for CHASM-TMB originate from the CH domain since they were located in the same position or in close approximation to the assigned signals of the isolated CH domain. The intense, unresolved signals that are absent from the original CH domain spectrum and appear around 8.5 ppm arise from the pxIDR region. Although only well-resolved signals were analyzable due to extensive overlap in the central region of the [^{1}H, ^{15}N]-HSQC spectrum, some chemical shift perturbations (CSPs) distinguished the spectrum collected for the CHASM-CH protein from that obtained from the CHASM-TMB protein. In this case, CSPs for many residues located within the CH domain in the vicinity of α-helices I, II, and III (particularly residues Glu-361, His-362, Lys-399, Arg-400, Arg-401, and Asn 403) and α-helix V (Arg-428) of the CH domain were identified (Figure 2A). Of these, Glu-361, His-362, Lys-399, Arg-400, and Arg-401 had CSP signals that persisted after titration with KCl; the other CSP signals were lost with increasing salt concentration (data not shown). These results suggest that intramolecular associations exist between the CH domain and pxIDR regions.

Further refinement of the residues involved in the intramolecular interaction between the IDR and CH domain was obtained by collecting the [^{1}H, ^{15}N]-HSQC spectrum of ^{15}N-CHASM-CH in the presence of unlabeled CHASM-pxIDR protein (Figure 2B). CSP values, determined from ^{15}N-labeled CHASM-CH following the addition of unlabeled CHASM-pxIDR, were plotted as a function of the residue number (Figure 2C). These CSPs are indicated in the [^{1}H, ^{15}N]-HSQC spectra (Figure 2B) and highlighted on the CH domain structure (Figure 2D). Amides that experience CSP > 0.15 were mapped to residues of the CH domain located between α-helix I and II (Glu-351, Trp-352, His-362, Phe-368), within α-helix VI (Asp-433, Lys-435, Tyr-438, Thr-439, Tyr-445, Arg-446) and within the C-terminal tail (Val-454, Lys-455, Thr-456, Lys-457, and Lys-458). Taken together, the results of the NMR

dx.doi.org/10.1021/bi2019018 | Biochemistry 2012, 51, 2694–2705

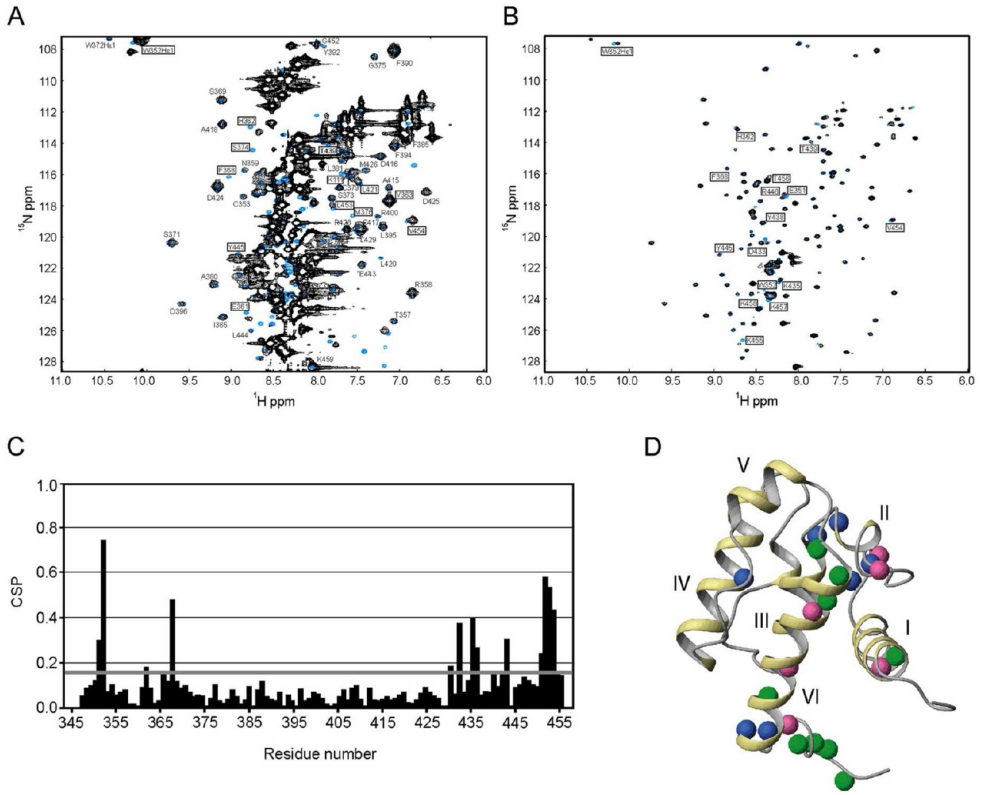

Figure 2. Intramolecular interface of the CH domain and the N-terminal intrinsically disordered region in CHASM-TMB as determined by NMR. In (A), the [^{1}H, ^{15}N]-HSQC spectrum for the isolated ^{15}N-CHASM-CH (cyan) and ^{15}N-CHASM-TMB (black) are shown. The backbone assignments for well-separated signals of the CH domain are indicated. The residues of the CH domain within the CHASM-TMB that exhibited chemical shift differences are boxed. In (B), due to the intense signals in the 8.5 ppm region, the [^{1}H, ^{15}N]-HSQC spectrum of ^{15}N-labeled CH domain in the presence of unlabeled CHASM-pxIDR was obtained. In (C), CSPs induced by CHASM-pxIDR binding to the isolated CHASM-CH domain are plotted as a function of the residue number. CSPs were calculated as a weighted average chemical shift difference of ^{1}H and ^{15}N chemical shifts. In (D), amide proton atoms with CSPs (>0.15) from panels (A) and (B) are mapped on the CHASM-CH structure as blue and green spheres, respectively, while those in common are mapped as pink spheres.

analyses suggest intramolecular associations between the CH domain and the pxIDR sequence of CHASM.

Protease Fragmentation and Hydrogen−Deuterium Exchange Mass Spectrometry Analysis of Intramolecular Interactions between the CH Domain and pxIDR of CHASM. Since two distinct regions of CHASM (one of which possesses significant structural disorder) were previously implicated in tropomyosin binding,[10] we employed hydrogen−deuterium exchange mass spectrometry (HDX-MS) approaches to maximize our structural resolution of the putative tropomyosin-binding surface. HDX-MS has been previously used to examine structural changes between intrinsically disordered and ordered states.[28,29] Protease digestion and HPLC separation conditions that produced CHASM peptide fragments of optimal size and distribution were established. These conditions resulted in overall detection of 65% of the amino acids (172 of 264) in the CHASM-TMB sequence, with redundant coverage of many areas within the protein (Figure 3A). The CH domain was mapped to 73% coverage, while the pxIDR was mapped to 60% coverage. A small area within the pxIDR (residues 259−319) contributed to the greatest gap in resolution, and this 60 amino acid-sequence is the most proline-rich section of CHASM. Additionally, four segments of the CH domain were unresolved. Peptides originating from an unstructured segment at the beginning of α-helix II (residues 369−378), and a small portion between α-helices IV and V (residues 418−420) were occasionally detected, but insufficient data were obtained for statistical analysis. A segment encompassing the entirety of helix III through to the N-terminal half of helix IV (residues 392−407) and a small segment of helix VI (residues 437−439) were also not detected.

The comparison of HDX-MS results for the CHASM-TMB (amino acids 196−459) and isolated CH domain (amino acids 345−459) revealed additional details of intramolecular interactions of the pxIDR with the CH domain (Figure 3B). A number of peptides from the CHASM-CH protein showed small decreases or no change in HDX when compared to the same peptides isolated from the CHASM-TMB. These data are indicative of a more "tightly" packed structure, and hence less HDX for the CH domain when removed from the pxIDR. Unfortunately, HDX results for amino acid residues Lys-399, Arg-400, Arg-401, and Asn-403 identified in NMR studies were not obtained. However, as shown in Figure 3B, Glu-361 and His-362 were contained in the peptide fragments MTRNYE (residues 356−361) and HVDIQN (residues 362−367), and Arg-428 was observed in the fragment VRLAVPDSKC (residues 427−436). The VRLAVPDSKC peptide showed significantly increased HDX in the presence of the pxIDR. Peptides containing residues Glu-361 and/or His-362 did not show any increase in exchange following the removal of the pxIDR sequence. Also of significance, the peptide LEWCRA (amino acids 350−355), which also contained amino acids (Glu-351 and Trp-352) identified by NMR as participating in

dx.doi.org/10.1021/bi2019018 | *Biochemistry* 2012, 51, 2694−2705

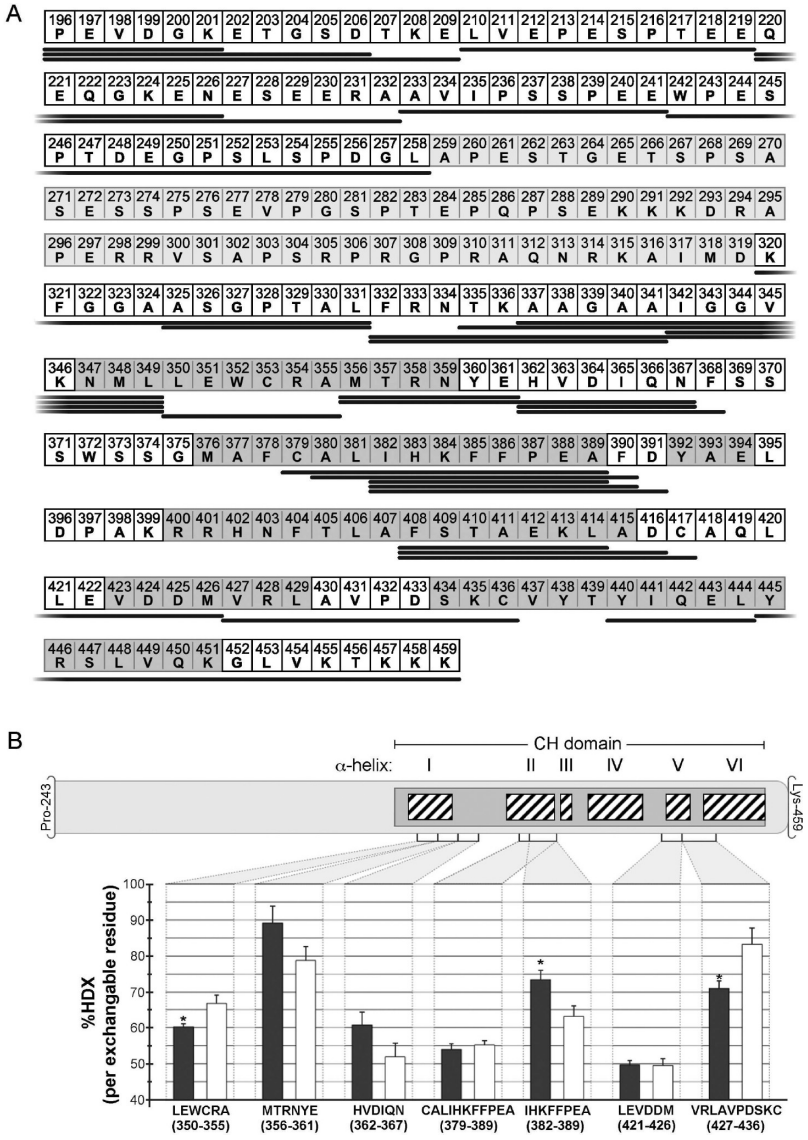

Figure 3. Intramolecular interface of the CH domain and the N-terminal intrinsically disordered region in CHASM-TMB as determined by HDX-MS. In (A), the mass spectrometric coverage for the peptic digest of CHASM-TMB is shown. Fragments were generated by "online" pepsin digestion. Black lines indicate the peptides routinely identified by LC-MS/MS analysis. The light gray highlighted region from residues Ala-259 to Asp-319 represents a contiguous segment (a proline-rich sequence encompassing the Ser-301 phosphorylation site) that could not be resolved. Helices within the isolated CH domain as determined by NMR[15] are shaded in dark gray. In (B), HDX-MS results are presented for peptides within the CH domain that may be involved in intramolecular binding of the pxIDR. The position of the peptide in the sequence of CHASM is depicted. The percent hydrogen−deuterium exchange (%HDX) is graphed for each peptide, where the solid and open bars indicate the %HDX obtained for the CHASM-TMB and CHASM-CH proteins, respectively. * − significantly different from corresponding %HDX obtained with CHASM-CH (Student's t test; $p < 0.05$; $n = 4-10$ separate determinations).

intramolecular binding, showed an increase in exchange with the removal of the pxIDR.

Determination of CHASM-Tropomyosin Binding Surfaces by NMR. When the [^{1}H, ^{15}N]-HSQC spectrum of CHASM-TMB was collected in the presence of tropomyosin, most signals from the CH domain disappeared upon titration with tropomyosin (Figure 4A, panels i and ii). The loss of signals may result from the fast relaxation due to the large molecular size of the complex (>90 kDa) or from the intermediate exchange rate in the NMR time scale that is expected from the determined K_D (i.e., 2×10^{-6} M). Although some signals from the pxIDR (i.e., residues 197−342) of the CHASM-TMB protein were shifted or disappeared upon addition of tropomyosin, most of them were still strong and remained in the same positions. Furthermore, when the KCl concentration was increased (Figure 4A; 100 mM, panel iii; 150 mM, panel iv), almost all the CH domain signals reappeared. This suggests that the higher salt concentrations could attenuate the binding affinity in a fast exchange manner within the NMR time scale; and therefore, the interaction was predominantly of an electrostatic nature.

Previous evidence suggests a role for the CHASM-CH domain in tropomyosin binding,[10] and the potential interaction was monitored in the ^{1}H, ^{15}N HSQC spectrum of CHASM-CH by adding unlabeled tropomyosin (Figure 4B). In this case, ^{15}N-CHASM-CH protein was used to limit the intense, unresolved signals that obscure CSPs elicited by interactions with tropomyosin. With the addition of tropomyosin (Figure

dx.doi.org/10.1021/bi2019018 | Biochemistry 2012, 51, 2694−2705

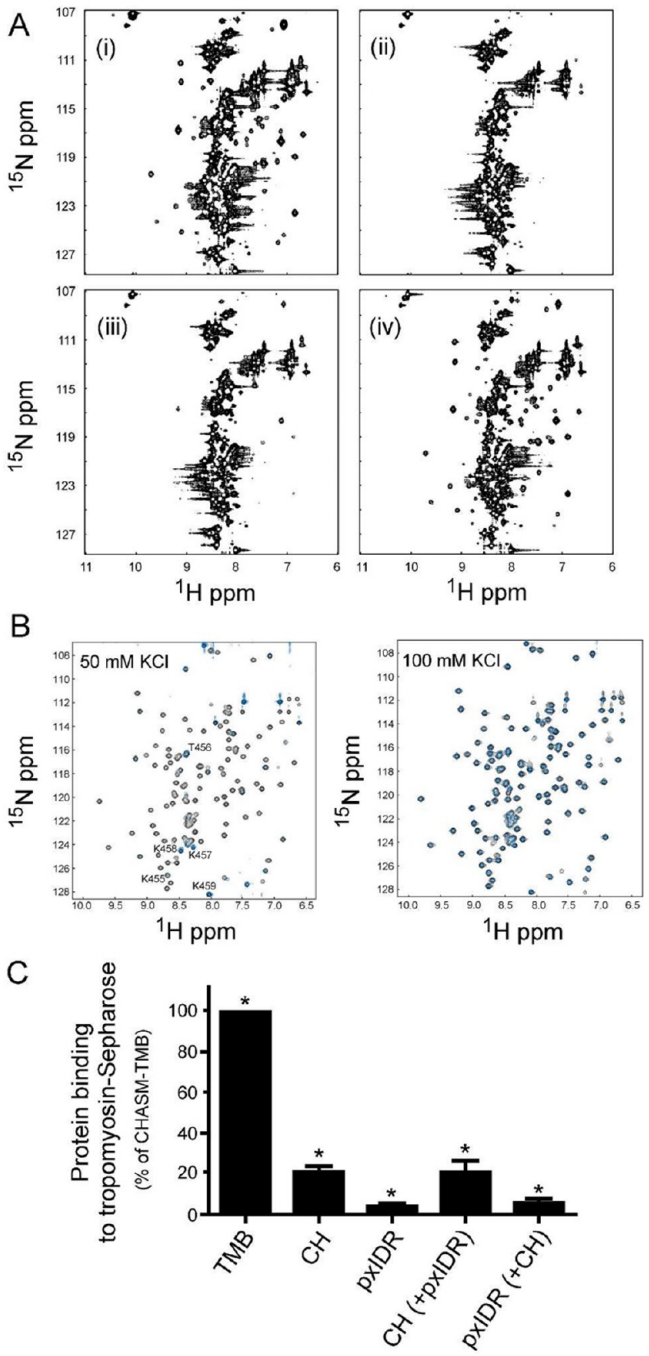

Figure 4. NMR and biochemical studies reveal CHASM-CH interactions with tropomyosin. In (A), the [^{1}H, ^{15}N]-HSQC spectra of ^{15}N-labeled CHASM-TMB in complex with unlabeled tropomyosin are presented. The HSQC spectrum of the free CHASM-TMB (i), CHASM-TMB in complex with tropomyosin with [KCl] of 50 mM (ii), 100 mM (iii), and 150 mM (iv). In (B), the HSQC spectrum for the isolated ^{15}N-labeled CHASM-CH (black) and ^{15}N-labeled CHASM-CH with tropomyosin (cyan) are shown for binding (50 mM KCl, left panel) and dissociating (100 mM KCl, right panel) conditions. In (C), tropomyosin-Sepharose was incubated with CHASM-TMB, CHASM-pxIDR, CHASM-CH or CHASM-CH plus CHASM-pxIDR protein. After 1 h incubation, the tropomyosin-Sepharose was washed to remove unbound protein. The amount of CHASM proteins associated with tropomyosin-Sepharose was determined by SDS–PAGE and densitometry. The relative ratio of CHASM protein pulled down with tropomyosin-Sepharose is shown with the binding of CHASM-TMB normalized to 100%. Mean values are reported with significant binding over blank-Sepharose indicated (*- Student's t test; $p < 0.05$; $n = 4$).

4B, left panel), most amide signals corresponding to residues in the CH domain disappeared due to increased correlation time. When KCl was increased to 100 mM to disrupt the interaction of the CH domain with tropomyosin, the majority of the signals reappeared (Figure 4B, right panel) with some broadening of signals detected. Taken together, the results of the NMR analyses suggest a prominent role for the CH domain in mediating the conformational dynamics of the tropomyosin-binding interface.

Experiments to examine the tropomyosin-binding potential of the individual CH domain and pxIDR were completed with biochemical pulldown using immobilized tropomyosin-Sepharose and sufficient CHASM protein to ensure stoichiometric binding (the reported K_D of the CHASM-TMB/tropomyosin complex being approximately 10^{-6} M[10]). As shown in Figure 4C, binding of the isolated CHASM-CH domain with tropomyosin was observed. Furthermore, a small, but significant, amount of CHASM-pxIDR was recovered. Although the % recovery of bound material was quite low when compared to CHASM-TMB, these binding events were significant when compared to those measured for control binding-reactions (i.e., blank-Sepharose). No increase in % binding was found when the pxIDR and CH domain were incubated together with tropomyosin-Sepharose.

Mapping Structural Alterations in CHASM upon Tropomyosin Binding with Hydrogen–Deuterium Exchange Mass Spectrometry. To help interpret the observed tropomyosin-induced conformational changes revealed by NMR analysis, we also examined HDX for each identifiable CHASM peptide as a function of tropomyosin binding (Figure 5A). The HDX results for all peptides were assembled and mapped onto the structure of CHASM-TMB (Figure 5B). Six peptides of CHASM-TMB had increased exchange after the introduction of tropomyosin. Four of these were located in the pxIDR (PEVDGKETGSD, residues 196–209; WPESPTDEGPSLSPDGL, residues 242–258; FRNTKAAGAA, residues 332–341; and FRNTKAAGAAIGGVKNML, residues 332–349), and two were located in the CH domain (LEVDDM, residues 421–426; and VRLAVPDSKC, residues 427–438). Two smaller redundant fragments IGGVKNML (residues 342–349) and PEVDGK (residues 196–201) did not show any statistically relevant change in deuteration upon binding of tropomyosin. This finding may indicate that the longer peptides FRNTKAAGAAIGGVKNML and PEVDGKETGSD demonstrated an increase in exchange resulting from changes in the FRNTKAAGAA and ETGSD sequences, respectively. This supposition is subject to the caveat that differing back-exchange rates for the digested peptides may interfere with the validity of comparisons of different digestion products. Only three peptides were noted to decrease in exchange by a statistically significant amount when CHASM-TMB was bound to tropomyosin: LEWCRA (residues 350–355), CALIHKFFPEA (residues 379–38), and ALIHKFFPEAF (residues 380–390). Although CALIHKFFPEA and ALIHKFFPEAF (which cover overlapping regions of the protein) decrease in exchange, a smaller peptide in the same region (IHKFFPEAF, residues 382–390) exhibited no significant change upon binding to tropomyosin. It is possible that, within this region, only the

dx.doi.org/10.1021/bi2019018 | Biochemistry 2012, 51, 2694–2705

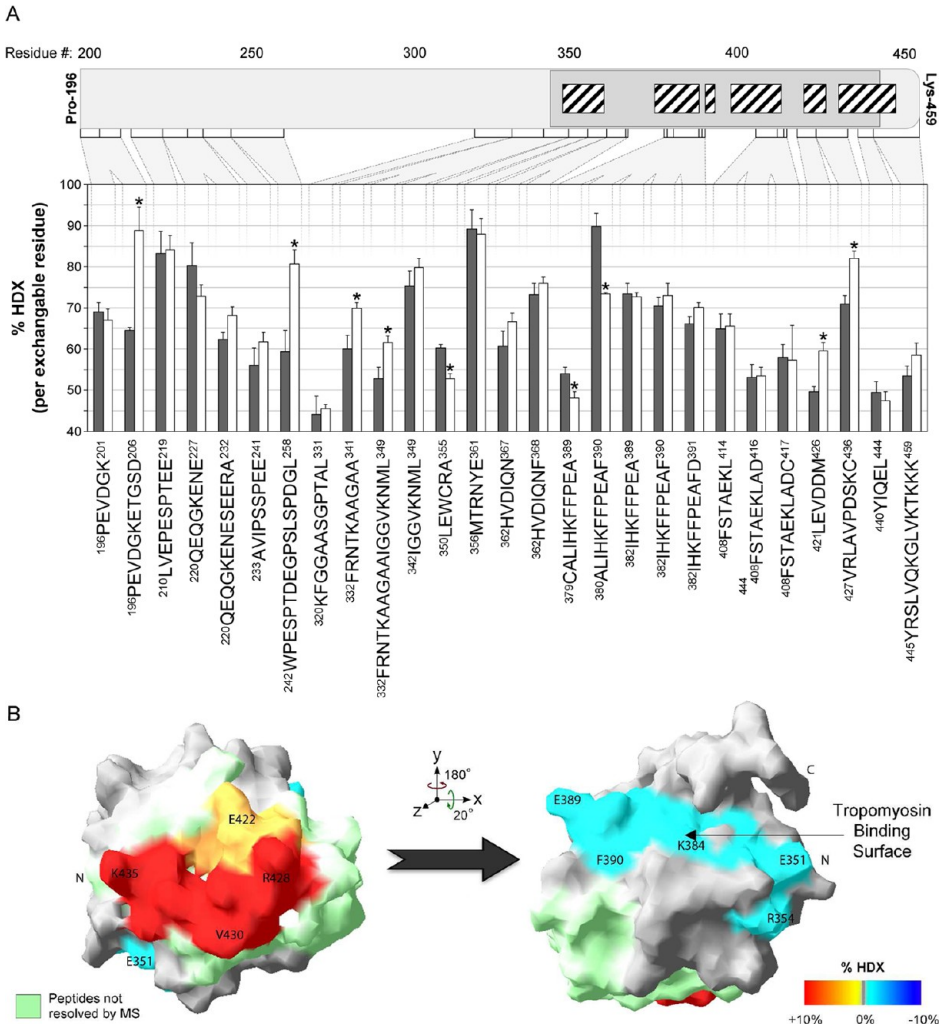

Figure 5. HDX-MS results suggest a tropomyosin-binding interface for the CH domain of CHASM. In (A), the relative position of each peptide within the CHASM-TMB sequence is depicted. Helices within the CH domain (dark gray box) as determined by NMR[15] are indicated with hatched boxes. The percent hydrogen−deuterium exchange (%HDX) is provided in the absence (solid bars) or presence (open bars) of tropomyosin. * − significantly different from corresponding %HDX obtained in the absence of tropomyosin (Student's t test; $p < 0.05$; $n = 6$−15 separate determinations). In (B), HDX data are plotted over the structure of the CHASM CH domain with some residues labeled for orientation. The heat map shows regions within the CH domain of CHASM-TMB after tropomyosin binding. Increased and decreased HDX induced by tropomyosin binding are represented by red and blue, respectively. Decreased HDX is representative of the tropomyosin-binding interface. Green regions indicate peptides that were not resolved by MS. The N- and C-terminal residues of the CH domain are indicated with (N) and (C), respectively.

CAL residues (residues 379−382) were affected by tropomyosin binding.

DISCUSSION

The CHASM protein is the newest member of the smoothelin family of muscle proteins that collectively provide important contributions to the contractile process.[4−6,11,13] The smoothelin family members are hypothesized to belong to a smooth muscle tropomyosin-troponin-like system,[3,5] and data have identified interactions with key structural proteins comprising the thin-filament. Indeed, our previous study provides evidence for an interaction of CHASM with tropomyosin;[10] however, we now provide several new insights into the structure of CHASM that reveal information on the interactions of the intrinsically disordered region with the globular CH domain and the engagement of these domains for tropomyosin binding.

Thus far, examinations of CHASM have provided a structure of the globular CH domain,[15] but details about the structure of the IDR at single residue resolution have not been forthcoming. Herein, we report that a significant amount of the CHASM protein sequence possesses intrinsic disorder. Specifically, our in silico examinations predicted an unstructured protein fragment for CHASM-IDR (residues 1−313), and in vitro spectroscopic analyses offered experimental confirmation of these predictions. The far-UV CD spectra also display low elliptical content for the CHASM-pxIDR that is consistent with that of disordered proteins.[30] Moreover, amide proton chemical shifts of residues in the N-terminal region of CHASM-TBD were poorly dispersed (6.5−8.5 ppm) in the two-dimensional NMR spectrum. Although the entire IDR of CHASM shares <10% similarity with the smoothelins, close inspection of the primary sequence alignments has revealed a set of spatially arranged amino acids that are conserved in the CHASM and smoothelin proteins.[1] The conserved primary sequence motif consists of clusters of basic and acidic amino acids distributed throughout the entire protein sequence. This novel motif was only revealed within the smoothelins due to nonconserved amino acid sequences in the intervening sequences of CHASM.

dx.doi.org/10.1021/bi2019018 | Biochemistry 2012, 51, 2694−2705

To assign some preliminary functionality to the CHASM motif, we searched the annotated protein databases with the primary amino acid sequence using PSI-BLAST and LigBase algorithms.[31] This search revealed a conservation of structural elements in the IDR between CHASM and the myristoylated, alanine-rich C-kinase substrate (MARCKS) family of proteins (i.e., the MARCKS-related protein (MRP) and MARCKS protein (MACS)). Intriguingly, the MARCKS proteins have been proposed to regulate actin structure at the plasma membrane interface[32,33] and assume nonhelical conformations with significant intrinsic disorder in solution.[34,35] Although the structural alignments revealed by the LigBase algorithms are weak, these data indicate that CHASM, MARCKS proteins and possibly the other smoothelin family members may have evolved thin filament interaction motifs from a similar archetype.

Whether the N-terminal IDR of CHASM possesses any microdomains of stable structure is unknown; however, several amino acids within α-helices I, II, and V of the CH domain were found by NMR to contribute to intramolecular associations with the pxIDR. Peptides containing a number of these residues (Glu-351, Trp-352, Glu-361, His-362, and Arg-428) were also resolved with HDX-MS. While peptides containing residues Glu-361 and His-362 did not exhibit increased HDX following the removal of the IDR, it is possible that any increases in HDX for Glu-361/His-362 due to the removal of the pxIDR from the CH domain were masked by decreases in exchange for other residues within the peptide. In conjunction with the NMR data, the involvement of the Arg-428 residue within the VRLAVPDSKC peptide (α-helix V; residues 427−436) to the intramolecular association can be reasonably concluded. In addition, a significant increase in HDX (i.e., solvent exposure) for the LEWCRA peptide (α-helix 1; residues 350−355) was revealed for the peptide upon deletion of the pxIDR. The results support the persistence of intramolecular interactions and suggest that the conformation of the CH domain is dependent on the presence of the pxIDR. The findings offer an explanation for why the isolated CH domain without the pxIDR was only capable of binding tropomyosin very weakly under NMR conditions.

These findings were recapitulated in biochemical experiments using chemical cross-linking. Cross-linking experiments (Supplementary Figure 3, Supporting Information) were performed to examine intramolecular associations. Cross-linking of CHASM-CH or CHASM-pxIDR produced only the two expected monomers, and spurious bands resulting from homodimer formation were not detected. When CHASM-CH was mixed with CHASM-pxIDR, a band of higher molecular mass was produced that had the mobility expected of the pxIDR-CH domain cross-linked complex. Although very modest levels of this complex were detected, this might be ascribed to a weak affinity introduced by severing the continuity of the polypeptide. On the basis of cross-linking, NMR and HDX-MS data, it seems likely that an intramolecular interaction exists. A reasonable model for how intramolecular associations might stimulate tropomyosin binding could involve independent yet cooperative interactions between the two structurally distinct regions. Unfortunately, our biochemical efforts to resolve the importance of the intramolecular interaction with respect to tropomyosin binding were ineffective. While it appeared that the CH domain and pxIDR could independently bind to tropomyosin, pull down experiments that contained the isolated CH domain plus pxIDR failed to provide clear-cut results for cooperation, presumably because this type of experiment requires the protein−protein complex to remain stable for the duration of the washing and capture steps.

Structural disorder confers many advantages on proteins (reviewed in ref 36) such as an increased speed of interaction, an increase in binding specificity without excessive binding strength, and an adaptability in binding that results from the protein's ability to fluctuate over an ensemble of structural states. And, many IDRs provide weak or transient molecular recognitions (i.e., with K_D values in the 10^{-3}−10^{-6} M range) with disorder-to-order transitions induced upon contact with the binding partner.[37] Indeed, the interaction of CHASM-TMB with tropomyosin can be characterized by weak binding ($K_D \sim 10^{-6}$ M).[10] During the course of these structural examinations, we have also revealed the dissociation of CHASM-TMB from tropomyosin under low salt conditions (i.e., 100 mM KCl). Furthermore, our biochemical pull-down approaches were successful in identifying weak interactions of CHASM-CH and CHASM-pxIDR with tropomyosin-Sepharose. While some might speculate as to the existence or functional relevance of weak protein−protein interactions in living cells, a number of studies are now revealing the underlying functional and structural principles of these weak (transient) protein−protein interactions (reviewed in refs 38−40). The detailed investigation of many potentially important transient (weak) complexes has been hindered since these protein−protein interactions are not amenable to verification by common biochemical methods, such as coimmunoprecipitation, pull-down and/or colocalization experiments.

Many studies have demonstrated disorder−order transitions within proteins upon ligand binding,[41] and many proteins possess significant intrinsic disorder to enable contacts with diverse arrays of interaction partners.[42,43] A number of proteins are known to bind tropomyosin, and functional analyses indicate binding modalities that typically involve disordered or partially folded domains. For example, the tropomyosin-binding domain of tropomodulin (Tmod; residues 1−92) is mainly disordered with only one short α-helical region (11 residues) with coiled-coil propensity.[44,45] Although not as comprehensively examined, the C-terminus of the polycystin-2 protein (a calcium-permeable cation channel) can also interact with tropomyosin, and multidimensional NMR methods provided backbone and side chain resonances for the domain that were typical of a partially folded protein.[46] For Tmod, a portion of the tropomyosin-binding domain became more ordered upon ligand binding (a peptide containing the N-terminus of α-tropomyosin),[45] and mutation of hydrophobic residues to negate α-helix or coiled-coil propensity was associated with a loss of binding.[44] In the case of CHASM, NMR data were unable to resolve whether tropomyosin-binding could induce structure within the IDR. But with the HDX-MS analysis, more peptides in the IDR from the CHASM-TMB protein were found to increase in exchange, indicating the loss or weakening of hydrogen bonds or at least an increase in solvent penetration. In binding studies, HDX-MS typically identifies regions of decreased exchange with the addition of a binding partner.[47] These regions have decreased solvent exposure and potentially increased local hydrogen bonding and are therefore considered to be sites of intermolecular interactions. From these results, we may infer that some structural rearrangement of the pxIDR occurs upon binding of tropomyosin to CHASM; however, it is apparent that the majority of the CHASM protein

remained highly disordered in solution even when associated with tropomyosin.

Using biochemical pull-down assays, we previously demonstrated that the globular CH domain was required for the interaction of CHASM-TMB with tropomyosin.[10] Although the CH domain can independently bind to tropomyosin in the NMR conditions (albeit very weakly), we propose herein that intramolecular engagements between the CH domain and pxIDR enable the binding of tropomyosin. When CHASM-TMB and tropomyosin were introduced, two of six peptides associated with increased HDX were located in the CH domain. These peptides are sequential to each other, comprising together the sequence LEVDDMVRLAVPDSKC (residues 421−436) that encompass the entirety of α-helix V and the beginning of α-helix VI. A couple of observations are significant regarding the increased exchange in this area. First, the Arg-428 residue was identified by NMR to be involved in the intramolecular interaction of CH domain with the pxIDR. Support for this finding was also offered with HDX-MS experiments for the VRLAVPDSKC peptide. Second, the increased exchange shown for the peptide after binding to tropomyosin suggests that increased flexibility in the pxIDR is introduced as a result of the binding. This hypothesis is favored by the qualitative observation that the exchange difference in VRLAVPDSKC caused by tropomyosin binding is about equal to that caused by truncation of the IDR. In a more general sense, the peptides detected from the pxIDR revealed a predilection for increased exchange, which could be explained by a model featuring a shift to a more flexible structure with increased solvent penetration for the IDR following tropomyosin binding.

Under tropomyosin-binding conditions, two CHASM-TMB peptides (LEWCRA and CALIHKFFPEA) exhibited decreased HDX and originate from within the CH domain. The LEWCRA peptide is an exposed sequence located on α-helix 1, at the beginning of the CH domain. The peptide revealed a significant increase in solvent exposure (i.e., HDX) with the removal of the IDR, which suggests that its conformation is dependent on the presence of the pxIDR. This offers an explanation for why the isolated CH domain without the pxIDR (and *vice versa*) was only capable of binding tropomyosin weakly. The latter portion of the putative binding region, CALIHKFFPEA, is also exposed and comprises the majority of α-helix II; however, the IHKFFPEA region of the peptide was independently detected and not observed to change in exchange by any significant amount. The remaining amino acids (i.e., CAL) are buried inside the globular structure of the CH domain; and therefore, it is unlikely that this surface was directly involved in tropomyosin binding. It is more plausible that the CAL sequence is in a portion of the interior of the CH domain that becomes compressed due to conformational shifts induced by tropomyosin binding, reducing solvent access to the region. Taking into consideration (1) the statistical relevance of the decreased exchange observed on this surface following the introduction of tropomyosin, (2) the effect of pxIDR removal on HDX for the LEWCRA peptide, (3) the amino acid composition, and (4) the relative exposure to solvent and therefore access to potential binding targets, it appears likely that the surface generated by the LEWCRA and CALIHKFFPEA peptides is principally involved in tropomyosin binding.

It is likely that additional, as yet undetected regions, of CHASM contribute to tropomyosin binding. This possibility is exemplified by the results of biochemical pull-downs of CHASM-CH and CHASM-pxIDR with tropomyosin-Sepharose. Other binding surfaces could be located in the proline-rich region encompassing residues 259−319 that was not resolved with pepsin digestion and HDX-MS. Notably, this region (unlike LEWCRA) is not conserved in the smoothelins and could offer an explanation for why smoothelin and CHASM do not share a single thin-filament binding mechanic. The thin filament localization properties of smoothelin were dependent on a region located well upstream of the CH domain and not conserved in CHASM.[8] In addition, the data suggest that the C-terminal tail of CHASM (i.e., KTKKK sequence) may not be involved in the interaction with tropomyosin since signals for these residues were still visible in binding conditions. The latter result is of particular significance given that this region was implicating in the association of apo-calmodulin with the CH domain.[15] Further experimentation will be required to identify if CHASM is able to bind tropomyosin and calmodulin simultaneously.

Several new conclusions emerge from our structural analysis of the tropomyosin-binding properties of CHASM. The structural nature of the intrinsically disordered region (IDR) of CHASM is poorly understood when compared to the remainder of the protein, and our studies provide evidence that a portion of the pxIDR forms intramolecular contacts with the CH domain. The results offer an explanation for why the isolated CH domain without the pxIDR was only capable of binding tropomyosin very weakly. Ultimately, intramolecular cooperativity between these structurally dissimilar regions is likely to provide an optimal binding surface for the tropomyosin interaction with the CH domain. The conformation of the CH domain appears to be dependent upon the presence of the pxIDR, and structural rearrangements within both CH and pxIDR domains may be necessary for positioning of the CHASM protein on thin filaments. Ultimately, it appears that the type-2 CH domain of CHASM is required for tropomyosin binding and presents a novel function for this protein domain.

■ ASSOCIATED CONTENT

Supporting Information

Additional details for (1) the expression of CHASM protein variants used in the studies, (2) the automated workflow for sample processing in the HDX-MS investigations, and (3) the results of chemical cross-linking to identify intramolecular associations are provided. This material is available free of charge via the Internet at http://pubs.acs.org.

■ AUTHOR INFORMATION

Corresponding Author

*Tel.: (403) 210-8433; fax: (403) 270-2211; e-mail: jmacdo@ucalgary.ca.

Author Contributions

#These authors contributed equally to this work.

Funding

The work was supported by research grants from the Canadian Institutes of Health Research (to H.J.V. and J.A.M.). A.U.L. holds a Heart & Stroke Foundation of Canada Fellowship. H.J.V. holds an Alberta Innovates − Health Solutions (AIHS) Scientist award. J.A.M. holds a Canada Research Chair (Tier II) and an AIHS Senior Scholar award.

Notes

The authors declare no competing financial interest.

■ ABBREVIATIONS

CD, circular dichroism; CH, calponin homology; CHASM, calponin homology-associated smooth muscle protein; CSP, chemical shift perturbation; HSQC, heteronuclear single quantum correlation; GST, glutathione-*S*-transferase; HDX, hydrogen−deuterium exchange; IDR, intrinsically disordered region; MS, mass spectrometry; PAGE, polyacrylamide gel electrophoresis; px, proximal; TMB, tropomyosin-binding region

■ REFERENCES

(1) Borman, M. A., MacDonald, J. A., and Haystead, T. A. (2004) Modulation of smooth muscle contractility by CHASM, a novel member of the smoothelin family of proteins. *FEBS Lett. 573*, 207−213.

(2) Kramer, J., Quensel, C., Meding, J., Cardoso, M. C., and Leonhardt, H. (2001) Identification and characterization of novel smoothelin isoforms in vascular smooth muscle. *J. Vasc. Res. 38*, 120−132.

(3) van Eys, G. J., Niessen, P. M., and Rensen, S. S. (2007) Smoothelin in vascular smooth muscle cells. *Trends Cardiovasc. Med. 17*, 26−30.

(4) Niessen, P., Rensen, S., van Deursen, J., De Man, J., De Laet, A., Vanderwinden, J. M., Wedel, T., Baker, D., Doevendans, P., Hofker, M., Gijbels, M., and van Eys, G. (2005) Smoothelin-a is essential for functional intestinal smooth muscle contractility in mice. *Gastroenterology 129*, 1592−1601.

(5) Rensen, S. S., Niessen, P. M., van Deursen, J. M., Janssen, B. J., Heijman, E., Hermeling, E., Meens, M., Lie, N., Gijbels, M. J., Strijkers, G. J., Doevendans, P. A., Hofker, M. H., De Mey, J. G., and van Eys, G. J. (2008) Smoothelin-B deficiency results in reduced arterial contractility, hypertension, and cardiac hypertrophy in mice. *Circulation 118*, 828−836.

(6) Wooldridge, A. A., Fortner, C. N., Lontay, B., Akimoto, T., Neppl, R. L., Facemire, C., Datto, M. B., Kwon, A., McCook, E., Li, P., Wang, S., Thresher, R. J., Miller, S. E., Perriard, J. C., Gavin, T. P., Hickner, R. C., Coffman, T. M., Somlyo, A. V., Yan, Z., and Haystead, T. A. (2008) Deletion of the protein kinase A/protein kinase G target SMTNL1 promotes an exercise-adapted phenotype in vascular smooth muscle. *J. Biol. Chem. 283*, 11850−11859.

(7) Niessen, P., Clement, S., Fontao, L., Chaponnier, C., Teunissen, B., Rensen, S., van Eys, G., and Gabbiani, G. (2004) Biochemical evidence for interaction between smoothelin and filamentous actin. *Exp. Cell Res. 292*, 170−178.

(8) Quensel, C., Kramer, J., Cardoso, M. C., and Leonhardt, H. (2002) Smoothelin contains a novel actin cytoskeleton localization sequence with similarity to troponin T. *J. Cell. Biochem. 85*, 403−409.

(9) van der Loop, F. T., Schaart, G., Timmer, E. D., Ramaekers, F. C., and van Eys, G. J. (1996) Smoothelin, a novel cytoskeletal protein specific for smooth muscle cells. *J. Cell Biol. 134*, 401−411.

(10) Ulke-Lemee, A., Ishida, H., Borman, M. A., Valderrama, A., Vogel, H. J., and MacDonald, J. A. (2010) Tropomyosin-binding properties of the CHASM protein are dependent upon its calponin homology domain. *FEBS Lett. 584*, 3311−3316.

(11) Lontay, B., Bodoor, K., Weitzel, D. H., Loiselle, D., Fortner, C., Lengyel, S., Zheng, D., Devente, J., Hickner, R., and Haystead, T. A. (2010) Smoothelin Like 1 protein regulates myosin phosphatase targeting subunit 1 expression during sexual development and pregnancy. *J. Biol. Chem. 285*, 29357−29366.

(12) Bodoor, K., Lontay, B., Safi, R., Weitzel, D. H., Loiselle, D., Wei, Z., Lengyel, S., McDonnell, D. P., and Haystead, T. A. (2011) Smoothelin-like 1 protein is a bifunctional regulator of the progesterone receptor during pregnancy. *J. Biol. Chem. 286*, 31839−31851.

(13) Borman, M. A., Freed, T. A., Haystead, T. A., and MacDonald, J. A. (2009) The role of the calponin homology domain of smoothelin-like 1 (SMTNL1) in myosin phosphatase inhibition and smooth muscle contraction. *Mol. Cell. Biochem. 327*, 93−100.

(14) Gimona, M., Djinovic-Carugo, K., Kranewitter, W. J., and Winder, S. J. (2002) Functional plasticity of CH domains. *FEBS Lett. 513*, 98−106.

(15) Ishida, H., Borman, M. A., Ostrander, J., Vogel, H. J., and MacDonald, J. A. (2008) Solution structure of the calponin homology (CH) domain from the smoothelin-like 1 protein: a unique apocalmodulin-binding mode and the possible role of the C-terminal type-2 CH-domain in smooth muscle relaxation. *J. Biol. Chem. 283*, 20569−20578.

(16) Wang, C. L., and Coluccio, L. M. (2010) New insights into the regulation of the actin cytoskeleton by tropomyosin. *Int. Rev. Cell Mol. Biol. 281*, 91−128.

(17) Gunning, P., O'Neill, G., and Hardeman, E. (2008) Tropomyosin-based regulation of the actin cytoskeleton in time and space. *Physiol. Rev. 88*, 1−35.

(18) Grzesiek, S., Bax, A., Clore, G. M., Gronenborn, A. M., Hu, J. S., Kaufman, J., Palmer, I., Stahl, S. J., and Wingfield, P. T. (1996) The solution structure of HIV-1 Nef reveals an unexpected fold and permits delineation of the binding surface for the SH3 domain of Hck tyrosine protein kinase. *Nat. Struct. Biol. 3*, 340−345.

(19) Wishart, D. S., Bigam, C. G., Yao, J., Abildgaard, F., Dyson, H. J., Oldfield, E., Markley, J. L., and Sykes, B. D. (1995) ^{1}H, ^{13}C and ^{15}N chemical shift referencing in biomolecular NMR. *J. Biomol. NMR 6*, 135−140.

(20) Delaglio, F., Grzesiek, S., Vuister, G. W., Zhu, G., Pfeifer, J., and Bax, A. (1995) NMRPipe: a multidimensional spectral processing system based on UNIX pipes. *J. Biomol. NMR 6*, 277−293.

(21) Johnson, B. A. (2004) Using NMRView to visualize and analyze the NMR spectra of macromolecules. *Methods Mol. Biol. 278*, 313−352.

(22) Yuan, T., Walsh, M. P., Sutherland, C., Fabian, H., and Vogel, H. J. (1999) Calcium-dependent and -independent interactions of the calmodulin-binding domain of cyclic nucleotide phosphodiesterase with calmodulin. *Biochemistry 38*, 1446−1455.

(23) *The PyMOL Molecular Graphics System*, Version 1.4.1, Schrodinger, LLC, New York, www.pymol.org.

(24) Williams, R. M., Obradovi, Z., Mathura, V., Braun, W., Garner, E. C., Young, J., Takayama, S., Brown, C. J., and Dunker, A. K. (2001) The protein non-folding problem: amino acid determinants of intrinsic order and disorder. *Pac. Symp. Biocomput.*, 89−100.

(25) Ward, J. J., Sodhi, J. S., McGuffin, L. J., Buxton, B. F., and Jones, D. T. (2004) Prediction and functional analysis of native disorder in proteins from the three kingdoms of life. *J. Mol. Biol. 337*, 635−645.

(26) Jones, D. T. (1999) Protein secondary structure prediction based on position-specific scoring matrices. *J. Mol. Biol. 292*, 195−202.

(27) Hinz, U. (2010) From protein sequences to 3D-structures and beyond: the example of the UniProt knowledgebase. *Cell. Mol. Life Sci. 67*, 1049−1064.

(28) Selevsek, N., Rival, S., Tholey, A., Heinzle, E., Heinz, U., Hemmingsen, L., and Adolph, H. W. (2009) Zinc ion-induced domain organization in metallo-beta-lactamases: a flexible "zinc arm" for rapid metal ion transfer? *J. Biol. Chem. 284*, 16419−16431.

(29) Wilson, L. M., Mok, Y. F., Binger, K. J., Griffin, M. D., Mertens, H. D., Lin, F., Wade, J. D., Gooley, P. R., and Howlett, G. J. (2007) A structural core within apolipoprotein C-II amyloid fibrils identified using hydrogen exchange and proteolysis. *J. Mol. Biol. 366*, 1639−1651.

(30) Kjaergaard, M., Norholm, A. B., Hendus-Altenburger, R., Pedersen, S. F., Poulsen, F. M., and Kragelund, B. B. (2010) Temperature-dependent structural changes in intrinsically disordered proteins: formation of alpha-helices or loss of polyproline II? *Protein Sci. 19*, 1555−1564.

(31) Stuart, A. C., Ilyin, V. A., and Sali, A. (2002) LigBase: a database of families of aligned ligand binding sites in known protein sequences and structures. *Bioinformatics 18*, 200−201.

(32) Hartwig, J. H., Thelen, M., Rosen, A., Janmey, P. A., Nairn, A. C., and Aderem, A. (1992) MARCKS is an actin filament crosslinking protein regulated by protein kinase C and calcium-calmodulin. *Nature 356*, 618−622.
(33) Wohnsland, F., Schmitz, A. A., Steinmetz, M. O., Aebi, U., and Vergeres, G. (2000) Interaction between actin and the effector peptide of MARCKS-related protein. Identification of functional amino acid segments. *J. Biol. Chem. 275*, 20873−20879.
(34) Arbuzova, A., Schmitz, A. A., and Vergeres, G. (2002) Cross-talk unfolded: MARCKS proteins. *Biochem. J. 362*, 1−12.
(35) Matsubara, M., Yamauchi, E., Hayashi, N., and Taniguchi, H. (1998) MARCKS, a major protein kinase C substrate, assumes non-helical conformations both in solution and in complex with Ca2+-calmodulin. *FEBS Lett. 421*, 203−207.
(36) Hazy, E., and Tompa, P. (2009) Limitations of induced folding in molecular recognition by intrinsically disordered proteins. *ChemPhysChem 10*, 1415−1419.
(37) Dyson, H. J., and Wright, P. E. (2005) Intrinsically unstructured proteins and their functions. *Nat. Rev. Mol. Cell Biol. 6*, 197−208.
(38) Nooren, I. M., and Thornton, J. M. (2003) Diversity of protein-protein interactions. *EMBO J. 22*, 3486−3492.
(39) Nooren, I. M., and Thornton, J. M. (2003) Structural characterisation and functional significance of transient protein-protein interactions. *J. Mol. Biol. 325*, 991−1018.
(40) Vaynberg, J., and Qin, J. (2006) Weak protein-protein interactions as probed by NMR spectroscopy. *Trends Biotechnol. 24*, 22−27.
(41) Garza, A. S., Ahmad, N., and Kumar, R. (2009) Role of intrinsically disordered protein regions/domains in transcriptional regulation. *Life Sci. 84*, 189−193.
(42) Uversky, V. N. (2011) Multitude of binding modes attainable by intrinsically disordered proteins: a portrait gallery of disorder-based complexes. *Chem. Soc. Rev. 40*, 1623−1634.
(43) Mittag, T., Kay, L. E., and Forman-Kay, J. D. (2010) Protein dynamics and conformational disorder in molecular recognition. *J. Mol. Recognit. 23*, 105−116.
(44) Kostyukova, A. S., Rapp, B. A., Choy, A., Greenfield, N. J., and Hitchcock-DeGregori, S. E. (2005) Structural requirements of tropomodulin for tropomyosin binding and actin filament capping. *Biochemistry 44*, 4905−4910.
(45) Greenfield, N. J., Kostyukova, A. S., and Hitchcock-DeGregori, S. E. (2005) Structure and tropomyosin binding properties of the N-terminal capping domain of tropomodulin 1. *Biophys. J. 88*, 372−383.
(46) Schumann, F. H., Hoffmeister, H., Schmidt, M., Bader, R., Besl, E., Witzgall, R., and Kalbitzer, H. R. (2009) NMR-assignments of a cytosolic domain of the C-terminus of polycystin-2. *Biomol. NMR Assign. 3*, 141−144.
(47) Konermann, L., Pan, J., and Liu, Y. H. (2011) Hydrogen exchange mass spectrometry for studying protein structure and dynamics. *Chem. Soc. Rev. 40*, 1224−1234.